Memoirs of the Scientific Sections of the Romanian Academy
Tome XXXIX, 2016

COMPUTER SCIENCE

IMAGE RESOLUTION RELATED BEHAVIOR FOR IRIS IDENTIFICATION BASED ON COLOR FEATURES

ADRIAN CIOBANU, TUDOR BARBU and MIHAELA LUCA

Romanian Academy – Iaşi Branch, Institute of Computer Science, Iasi, Romania
Correspondig author: adrian.ciobanu@iit.academiaromana-is.ro

The most used approach for iris identification is based on analyzing its texture by methods introduced and refined by John Daugman. In order to obtain very good rates of correct identification, a relatively good iris image is required, *i.e.* the iris must have at least a radius of 70 pixels in a near-infrared monochrome image. In latest years, we have developed a method of extracting color features from color images based on the LAB color system. The method constructs complex histograms over the LAB color space, made of bins corresponding to optimized rectangular parallelepipeds. We tested our method to see the minimum acceptable radius of an iris image that can still be correctly identified in most of the cases. To this end, we degraded four times the very good iris images in the UPOL database. The results obtained over the five sets of images, with radii varying from 250 pixels to only 16 pixels for each iris, show that our method can produce very good identification results at iris radii as low as 32 pixels.

Keywords: iris identification, iris radius, texture, LAB color features, spatial information.

1. INTRODUCTION

The most frequently used approach for iris identification is based on analyzing its texture, according to methods introduced and refined by John Daugman [3–6]. In order to obtain very good rates of correct identification, a relatively good iris image is required, *i.e.* the iris must have at least a radius of 70 pixels in a near-infrared monochrome image, the range 100–140 pixels being recommended by the same author [5].

In latest years, we have developed a method of extracting color features from color images based on the LAB color system [1]. The method constructs complex histograms over the LAB color space, made of bins corresponding to optimized rectangular parallelepipeds. We have applied this method to iris identification through local color distribution, by taking LAB color features from up to 8 parts of an iris image. We obtained identification rates of up to 98.70% for the UPOL database, containing 384 very good color images, with iris radii in the range of 220–250 pixels.

In this paper, we explore how does the resolution of iris images influence the results of identification, based on our LAB color features method. In the following

section we describe the sets of images with different iris radii used in our tests. Then, in section 3 we detail the common iris identification procedure used on all the test sets of images. Section 4 presents and discusses the results of our tests and the paper ends with the conclusion section.

2. SETS OF IRIS IMAGES USED IN TESTS

All sets of images used in this paper are derived from the UPOL iris database [7–9], which contains 384 high-quality images belonging to 64 persons (3 images for each eye of each person). The images are of good resolution (576×768) and are coded in the PNG format with 24 bits of RGB color for each pixel. The eyes were scanned by a TOPCON TRC50IA optical device connected to a SONY DXC-950P 3CCD camera [7]. The results presented in [1] were obtained on a manually segmented set of 384 iris images, this time images being coded in the BMP format, with radii varying from 220 to 250 pixels. This set of iris images represent also the first set used for tests in the present paper, having an average number of 159,161 pixels per segmented iris image.

The second set was obtained from the first one by replacing every four pixels with one pixel having as RGB coefficients the average value of the RGB coefficients of the original four pixels. After cropping each original image to have a horizontal and vertical number of pixels multiple of 4, we have applied block operations available in MATLAB. For instance, for the red plane, we transform the original IR plane in the degraded IR1 by the following code:

```
media = @(x) uint8(mean(mean(x))); IR1 = blkproc(IR,[2,2],media);
```

The second set of iris images, obtained by this procedure, has iris radii ranging from 110 to 125 pixels, with an average number of 40,002 pixels per iris image. Applying the same procedure to the second set of iris images, we obtained the third one, with iris radii ranging from 55 to 63 pixels and an average number of 10,105 pixels per image. From the third set of images, we obtained the fourth set with iris radii, ranging from 22 to 32 pixels and an average number of 2,575 pixels per image. While not envisioned at the start of our tests, we had to consider a fifth set, with degraded images of only 665 pixels/image on the average, or iris radii as short as 11 to 16 pixels. Figure 1 show examples of corresponding degraded images for two segmented images of the original UPOL set. In order to observe the degradation level of each set, the images were scaled to the same size.

To produce the values needed to assess the minimum resolution of an iris image acceptable for its identification by using our LAB color features method, we have applied the same identification procedure to all five different sets of segmented iris images described above. The procedure consists in four steps: finding the optimized LAB bin limits, extracting the LAB color features, computing the distances between the feature vectors of all 384 images and identifying each iris image as pertaining to the person having the closest iris image to the one in question.

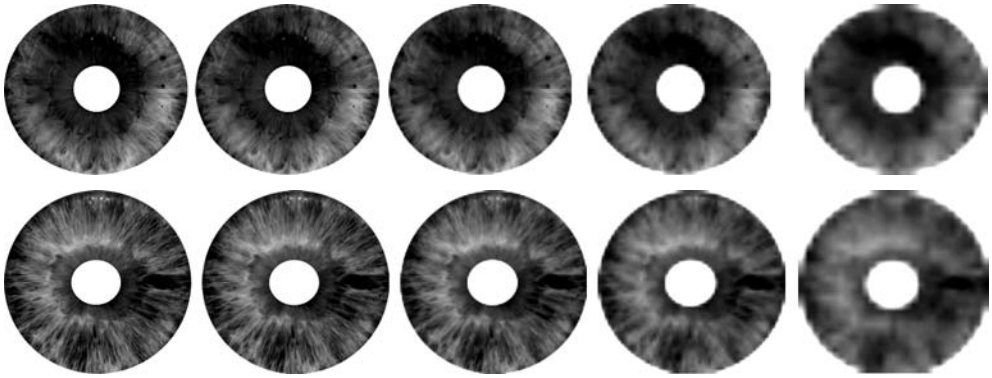

Fig. 1. Examples of degraded images belonging to the second, third, fourth and fifth set, arranged in order from left to right. The first image on the left is the original full resolution UPOL segmented image. Images shown here in gray levels are used in full color in tests.

3. COMMON IRIS IDENTIFICATION PROCEDURE

Considering that our LAB color features method allows different configurations [1], we choose to evaluate its behavior in three configuration cases: 5×4×4 = 80 color features/iris partition (which means a total of 640 color features for all 8 iris partitions we used in our tests, see Fig. 2), 4×3×3 = 36 color features/iris partition (a total of 288 color features) and 3×2×2 = 12 color features/iris partition (a total of 96 color features).

Fig. 2. Iris partitioned in 8 different regions. Color features are extracted for each of these partitions and then concatenated to produce the final feature vector for one iris.

Optimization of the LAB bin limits is done as presented in [2]. Basically, one has to input the configuration of the LAB color features extractor (like 4×3×3, which means that there are 4 partitions over the ***L*** axis, 3 partitions over the ***a*** axis and also 3 partitions over the ***b*** axis) and of the directory where the set of images are stored. The optimization routine reads all images, counts all different colors found inside them and produces the LAB bin limits so that each obtained

rectangular parallelepiped bin hosts almost the same number of pixels from the total number of pixels of all the 384 images in a set. Figure 3 plots the limits obtained for the 4×3×3 configuration and for all five sets of segmented iris images. As the resolution of images decreases, the limits are adapted and the bins become narrower, which is reasonable as the number of pixels per image also decreases dramatically.

Extraction of LAB color features is done as described in [1]. After computing the distances between all 384 iris images, a minimum distance classifier is applied to identify each iris image, based on the closest image from the other 383 images in their respective set.

```
LL(:) = [0 73 93 117 255];

La(:,1)=[109 148 152 190];
Lb(:,1)=[34 151 156 170];

La(:,2)=[105 140 147 200];
Lb(:,2)=[18 152 159 179];

La(:,3)=[97 136 140 199];
Lb(:,3)=[28 148 159 187];

La(:,4)=[62 134 136 214];
Lb(:,4)=[43 151 156 216];
```

```
LL(:) = [4 72 94 116 255];

La(:,1)=[119 148 152 179];
Lb(:,1)=[45 151 154 168];

La(:,2)=[118 140 147 194];
Lb(:,2)=[23 152 159 175];

La(:,3)=[102 136 140 197];
Lb(:,3)=[28 148 159 184];

La(:,4)=[70 134 136 207];
Lb(:,4)=[46 149 156 210];
```

```
LL(:)= [12 73 95 119 255];

La(:,1)=[124 148 152 173];
Lb(:,1)=[58 151 156 166];

La(:,2)=[121 138 148 176];
Lb(:,2)=[49 152 159 173];

La(:,3)=[116 134 139 184];
Lb(:,3)=[50 148 157 180];

La(:,4)=[94 132 137 188];
Lb(:,4)=[63 148 155 201];
```

```
LL(:)= [18 76 97 120 255];

La(:,1)=[128 148 150 164];
Lb(:,1)=[86 150 155 166];

La(:,2)=[125 137 146 167];
Lb(:,2)=[93 150 159 173];

La(:,3)=[126 134 140 170];
Lb(:,3)=[103 149 158 180];

La(:,4)=[110 132 135 172];
Lb(:,4)=[98 148 155 187];
```

```
LL(:)=[23 78 102 125 254];

La(:,1)=[131 147 150 162];
Lb(:,1)=[114 152 157 166];

La(:,2)=[129 138 145 163];
Lb(:,2)=[116 149 159 172];

La(:,3)=[128 135 139 163];
Lb(:,3)=[119 149 155 179];

La(:,4)=[125 132 134 162];
Lb(:,4)=[123 140 151 181];
```

Fig. 3. Optimized LAB bins for the original set of segmented iris images and the other four degraded sets in the case of 4×3×3 bins configuration.

4. RESULTS

The obtained results are presented in Figure 4. As the results in terms of identification percentage are in a close range, from the best situation, of 380 correctly identified irides with 98.96%, to the worst situation, of 367 correctly identified irides with 95.57%, we plotted directly on the graphic the number of correctly identified irides in each situation. There are 15 test results, three for each bin configuration applied on each of the five test image sets.

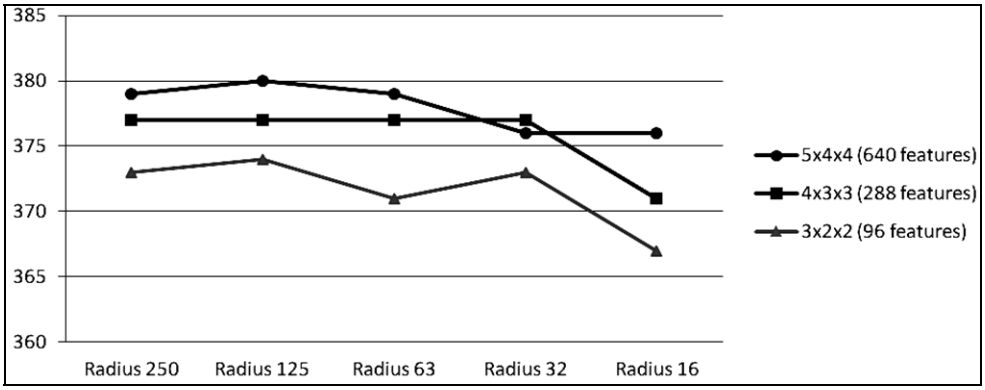

Fig. 4. Number of correctly identified irides (384 in total) by LAB bin configuration, for the original set of segmented iris images (radius around 250 pixels) and the subsequently degraded four sets (radius around 125, 63, 32 and 16 pixels).

The results show us that there might be an optimum resolution for the segmented iris images. We obtained the best identification result for two out of three bin configurations in the images where iris radii were around 125 pixels, better than with original radii around 250 pixels. This is a valuable result, exempting us from working with unnecessary big images, and thus saving computing time and storage capacity. For each application, it should be possible to find an optimum between the size of images and the identification rates.

Also, we can see that for the 4×3×3 bins configuration we obtained constant identification rates over a wide range (from radii around 250 pixels to radii around 32 pixels). So, it might be possible to find an optimum bin configuration for a given application of our method.

As for the minimum acceptable radii for an iris segmented image, we can see from Figure 4 that radii around 32 pixels are still suitable for obtaining high iris identification rates. This is lower than the 70 pixels radius stated by Daugman for his texture-based iris identification [5]. Moreover, even the identification rates at radii as low as 16 pixels are not so bad. If sufficient features are extracted, a very good identification rate of 97.79% can still be obtained.

These results make our method a good candidate for the identification of irides on the basis of low resolution pictures, like the ones obtained by surveillance cameras or smartphones.

5. CONCLUSIONS

In this paper we presented the results of tests run with our LAB color features identification method for segmented iris images, in cases where the radius of the iris is ranging from 250 pixels to 16 pixels. The tests were done to identify a minimum working radius, so that the identification rates remain sufficiently high. The results confirm that our method can be applied for iris images with radii well under the threshold of 70 pixels stated by Daugman [5] for his texture-based identification method. In fact, radii as low as 32 pixels are good enough, while some good results can be obtained even at radii as low as 16 pixels, provided that a sufficient number of color features is extracted. This makes our method a good candidate for the identification of irides on the basis of low resolution pictures, like the ones obtained by surveillance cameras or smartphones.

Authors' contributions*:* AC and ML had the idea behind this paper and designed the methodology; AC and TB implemented the methodology in MATLAB scripts and conducted experiments; AC and ML analyzed data; AC and TB wrote the paper; ML made corrections and revisions.

REFERENCES

1. CIOBANU A., LUCA M., PAVALOI I., *Iris Identification Based on Optimized LAB Histograms Applied to IRIS Partitions*, Buletinul Institutului Politehnic din Iasi, published by the "Gh. Asachi" Technical University, Tome **LX(LXIV)**, Fasc. I, 2014, Section Automatica si Calculatoare, 2014, 37-48, available online at www12.tuiasi.ro/users/103/Buletin_2014_1_37-8_3_Ciobanu_AC%201_2014.pdf.
2. CIOBANU A., PAVALOI I., LUCA M., MUSCA E., *Color Feature Vectors Based on Optimal LAB Histogram Bins*, 12th International Conference on Development and Application Systems, Suceava, Romania, May 2014, 15–17.
3. DAUGMAN J., *Biometric Personal Identification System Based on Iris Analysis*, US Patent 5291560, http://patft.uspto.gov/netacgi/5291560, 15 July 1991.
4. DAUGMAN J., *High Confidence Visual Recognition of Persons by a Test of Statistical Independence*, IEEE Transactions on Pattern Analysis and Machine Intelligence, November 1993, **15** (11), 1148−1161.
5. DAUGMAN J., *How Iris Recognition Works*, IEEE Transactions on Circuits and Systems for Video Technology, 2004, **11** (3), 21−30.
6. DAUGMAN J., *New Methods in Iris Recognition*, IEEE Trans. Systems, Man, Cybernetics B, 2007, **37** (5), 1167−1175.
7. DOBEŠ M., MACHALA L., TICHAVSKÝ P., POSPÍŠIL J., *Human Eye Iris Recognition Using the Mutual Information*, Optik, 2004, **115** (9), Elsevier, 399−405.
8. DOBEŠ M., MARTINEK J., SKOUPIL D., DOBEŠOVÁ Z., POSPÍŠIL J., *Biometric Personal Identification System Based on Iris Analysis*, Optik, 2006, **117** (10), Elsevier, 468−473.
9. DOBEŠ M., MACHALA L., *Iris Database*, http://www.inf.upol.cz/iris/ UPOL Iris Database, 2005, (Accessed 10 May 2013).

Received February 21, 2016